Phase Decomposition as a Hydrocarbon Indicator: A Case Study

Ramses Meza, Gerard Haughey, BHP Billiton, John Castagna, University of Houston, Umberto Barbato, Oleg Portniaguine, Lumina Geophysical*

Summary

Phase decomposition is applied to low-impedance hydrocarbon-bearing sands in a clastic section where sand thicknesses vary from the vicinity of tuning to well below tuning. In order to properly interpret seismic phase changes caused by the introduction of hydrocarbons, it is useful to artificially "thin" the targets by high-cut filtering the data, thereby increasing the tuning thickness and making more layers seismically thin. Once the seismic thinning is performed, the amplitudes separate into the expected phase components, resulting in a different spatial distribution of mapped amplitudes than on the original seismic data. A useful method to determine what frequencies are required to obtain proper phase separation in a section with stacked interfering sands, is to apply spectral decomposition to a synthetic seismogram, followed by phase decomposition.

Introduction

The use of phase decomposition as a direct hydrocarbon indicator was introduced by Castagna et al., (2016). This is based on the idea that, for thin layers, the "hydrocarbon effect" or change in amplitude caused by the addition of gas to a brine-filled layer, is -90 degrees phase-rotated with respect to the wavelet. Phase decomposition maps amplitude as a function of phase, resulting in phase "gathers". Phase filtering can then be performed by summing over specific "phase bands" to enhance events with desired phase or suppress events with the wrong phase to be of interest. In the case of thin low impedance gas-sands (bright spots), and with a zero phase wavelet, we expect the amplitude anomaly to be strongest on the -90 degree phase component. However, the amplitude/phase relationship is frequency dependent, so when dealing with targets of varying thickness in the vicinity of tuning, a combination of spectral decomposition and phase decomposition can be employed to optimize the phase and frequency for which amplitude anomalies should occur. For example, with a zero-phase wavelet, while a thin bright spot may show the hydrocarbon effect best on the -90 degree phase component, a layer above tuning with the same impedance will appear best on the -180 degree phase component. Thus, resolved layers will show little improvement with respect to a zero-phase seismic trace. Fortunately, a seismic layer can be artificially thinned by low-pass filtering. This allows the interpreter to study phase- and frequency-dependent amplitude anomalies. These ideas are illustrated on a 3D seismic dataset acquired over poorly consolidated clastic sediments containing low-impedance target sand reservoirs of varying thickness. The data is a far stack (31° to 45°) that has been zero-phased, so our expectation is for thin hydrocarbon bearing bright-spot reservoirs to be most anomalous on the -90 degree phase component.

Synthetic Modeling of Frequency and Phase Effects

While phase decomposition can be used as a reconnaissance tool, when a wide range of thicknesses are expected, the interpretation is clarified by synthetic modeling. Assuming that the data has been processed so that a simple convolutional model yields a good synthetic tie, the amplitude-phase-frequency relations are readily determined by performing spectral decomposition on the synthetic trace, followed by phase decomposition. With a zero-phase wavelet, the sum of zero and -180 degree phase components (referred to as "even") and the sum of -90 and +90 degree components (referred to as "odd") are particularly useful attributes. For thin layers exhibiting bright spots, we expect amplitude anomalies to be best on the odd component.

A real data case is illustrated in figure 1. Here, a synthetic trace is produced and spectral decomposition using the Continuous Wavelet Transform (CWT) is performed (e.g., Castagna and Sun, 2006). Phase decomposition is applied to the resulting frequency gather (labelled as input in figure 1) and the even and odd component outputs are displayed next to the input gather. It is observed that the phase components are frequency dependent. This frequency dependence is a consequence of varying layer thicknesses and interference between closely-spaced events. Three target intervals are evident on the well logs (labelled Events 1-3). These vary in thickness, and therefore, in spectral response. All of these are low impedance hydrocarbon bearing sands. For zero-phase calibrated data, the amplitude anomalies are expected to appear in the odd component. The tops (red dashed lines) and bases (blue dashed lines) of each target sand are highlighted in the figure. From this figure one can determine that the seismic dominant frequency needed to best 'illuminate' Event-1 and Event-2 (~20m thick) is 20-30 Hz, and for Event-3 (~7m) is between 25-45 Hz (black arrows). The synthetic gather response provides a guide regarding the expected seismic response of these target sands. Not taking into account the frequency dependency of these targets can lead to erroneous interpretations of the results. The original seismic has a dominant frequency between 40 and 50 Hz. This would be too high to observe the expected anomalous phase response for Events 1 and 2, which require lower frequency content in order to maintain the necessary thin layer condition. A high-cut filter is therefore applied in order to remove high frequencies to artificially ‘thin’ these layers. was also the prediction observed in the synthetic gather response.

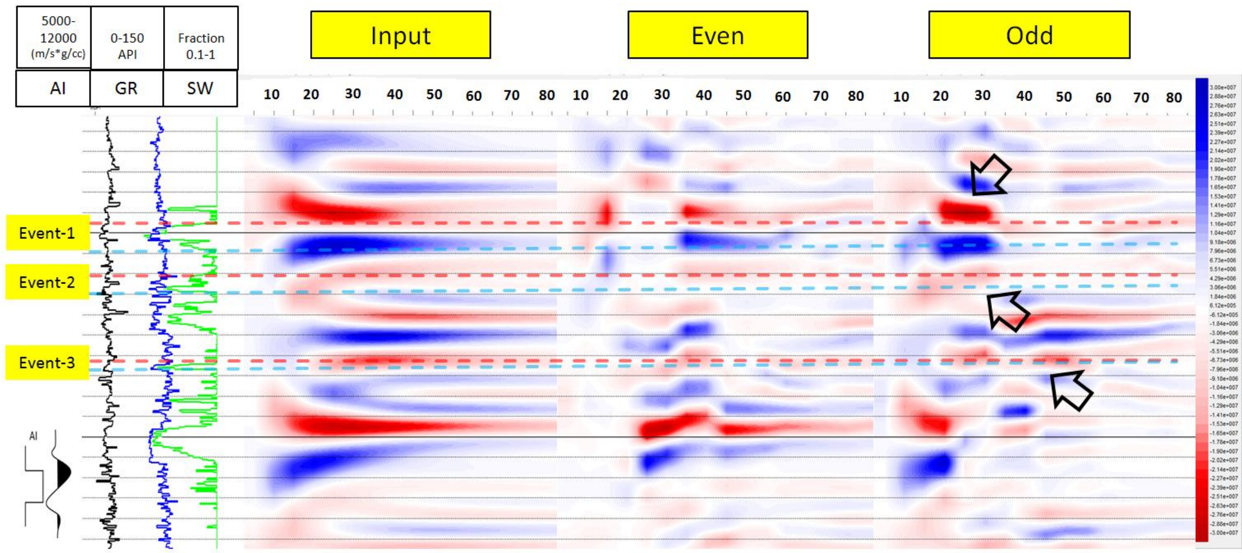

Figure 1. Phase Decomposition on a synthetic frequency gather. Black arrows show event’s illumination dominant frequency

Seismic Data Application

Phase Decomposition was applied to the original and high-cut filtered stacked seismic data (far stack). Figure 2 shows a time structure map for Event-1 in which an arbitrary line crosses the main structure.

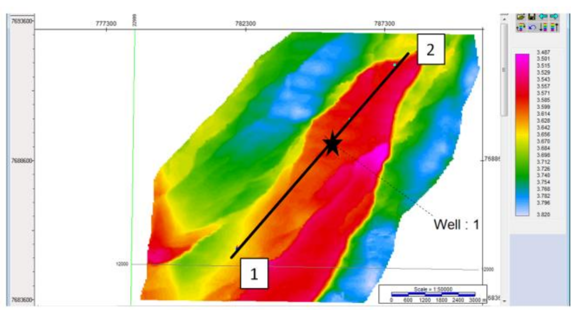

Figure 2. Time structure map of Event-1 showing the arbitrary line to be reviewed in vertical section.

The results of phase decomposition of the original dataset can be observed in figure 3. Event-1 exhibits a clear amplitude anomaly in the input data with the characteristics of a DHI. Event-3 also displays bright amplitudes. Event-2 is the least evident. The even component appears to retain the amplitudes of both Events-1 and 2. This, however, was expected, as these two layers are close to being resolved by the input seismic, violating the ‘thin layer’ prerequisite.

Event-3 shows a clear separation in both components, with the energy observed mainly in the odd component. This

Figure-4 shows a similar analysis applied to the high-cut filtered data. The difference is noticeable. The amplitudes corresponding to Events-1 and 2 have moved to the odd component. This also agrees with the results observed at the synthetic trace. The separation on Event-3 is also more evident. It is important to note that the generation of the phase components from seismic is independent of the wells. Windowed map extractions of the most negative amplitude are calculated (see figures 6 and 7). For Event-1 (figure 6abc), the even component dominates the amplitude anomalies of the input data. However, when high-cut filtered (figure 6def) there is a clear separation of the amplitudes between even and odd components. The northeast portion of the amplitude anomaly appears on the even component, while the southwest portion appears on the odd component. An unmapped fault separating these two different amplitude behaviors can be found on figure 4. It is evident that this novel style of amplitude interpretation can provide useful insights. Note that the artificial ‘seismic thinning’ was key in order to properly separate the amplitude anomalies. An interpretation solely based on the input data would have placed the anomalies mainly in the even component, which could have been interpreted as wet sand, lowering prospectivity in the area. Figure 7 shows similar findings for Event -2. Again, after the high-cut filter, the amplitudes of the pay sand move towards the odd component. Figure 5 shows a closer look of the extractions on the original data.

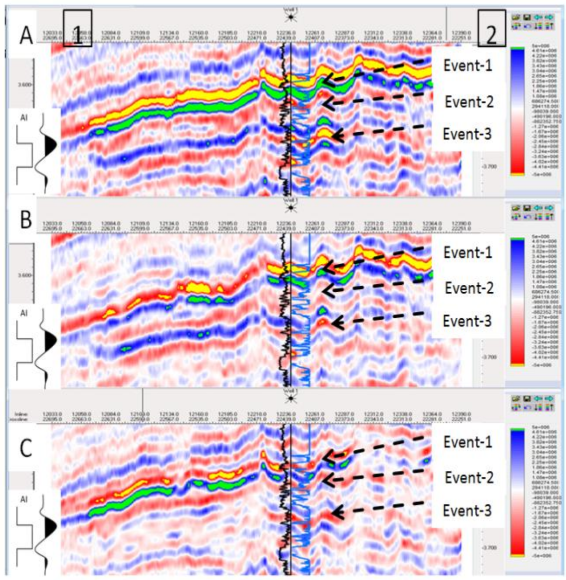

Figure 3. Vertical sections showing A) Input Data, B) Even Component, and C) Odd Component, of the original data. The displayed logs are Gamma Ray (black) and Water Saturation (blue).

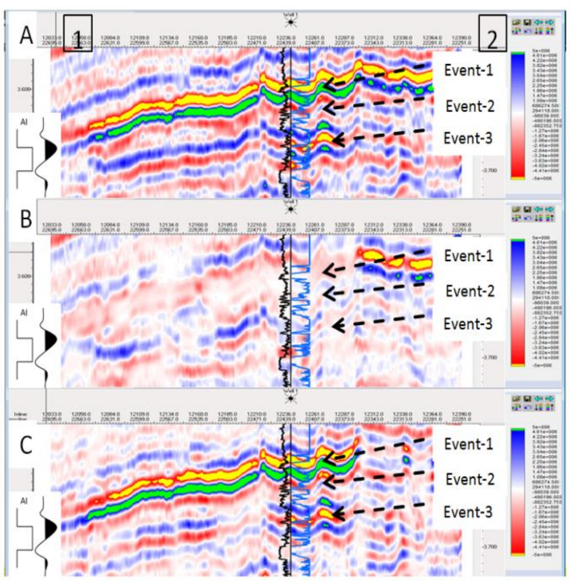

Figure 4. Vertical section showing A) Input Data, B) Even Component, and C) Odd Component, of the high-cut data.

(no bandpass filter was applied) for Event-3. The amplitude extraction of the input shows 3 main bright spots. Two of them remain similar after phase decomposition, but one is split into two anomalies in the even and odd components. The well crosses this amplitude anomaly in the odd component on a structural high (as observed in panel C).

Conclusions

Phase Decomposition provides additional insight into amplitude anomaly interpretation. Separating the seismic trace into phase-dependent even and odd components allows us to make inferences providing the interpreted layers are seismically thin. For layers above and in the vicinity of tuning, artificial "thinning" can be accomplished by spectral decomposition or simple high-cut filtering. Thin low-impedance gas bearing sands are best detected in the odd component when said layer is well below seismic resolution. Removing high frequencies via bandpass filtering allows us to thin layers that are otherwise resolved, achieving an optimal illumination frequency. The technique is independent of well control; however, well data can be used to calibrate the phase of the data (which is paramount to provide an accurate interpretation) and to model frequency gathers that can allow the interpreter to determine the frequency content necessary to tune each event. A good correlation between phase behavior of seismic and well data provides a degree of certainty and allows for more precise interpretation of the results.

Acknowledgments

The authors would like to thank BHP Billiton, Schlumberger and Lumina Geophysical for providing the data set and software for this project, as well as permission to publish this work.

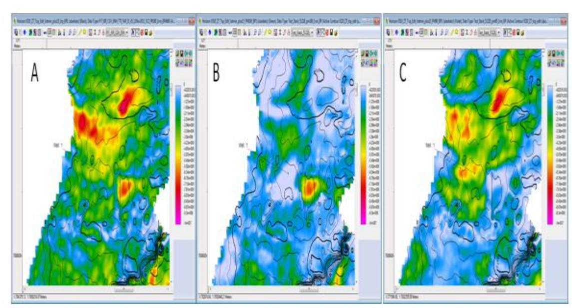

Figure 5. Map extraction for Event-3. Extractions are made in A) Input data, B) Even component, C) Odd Component.

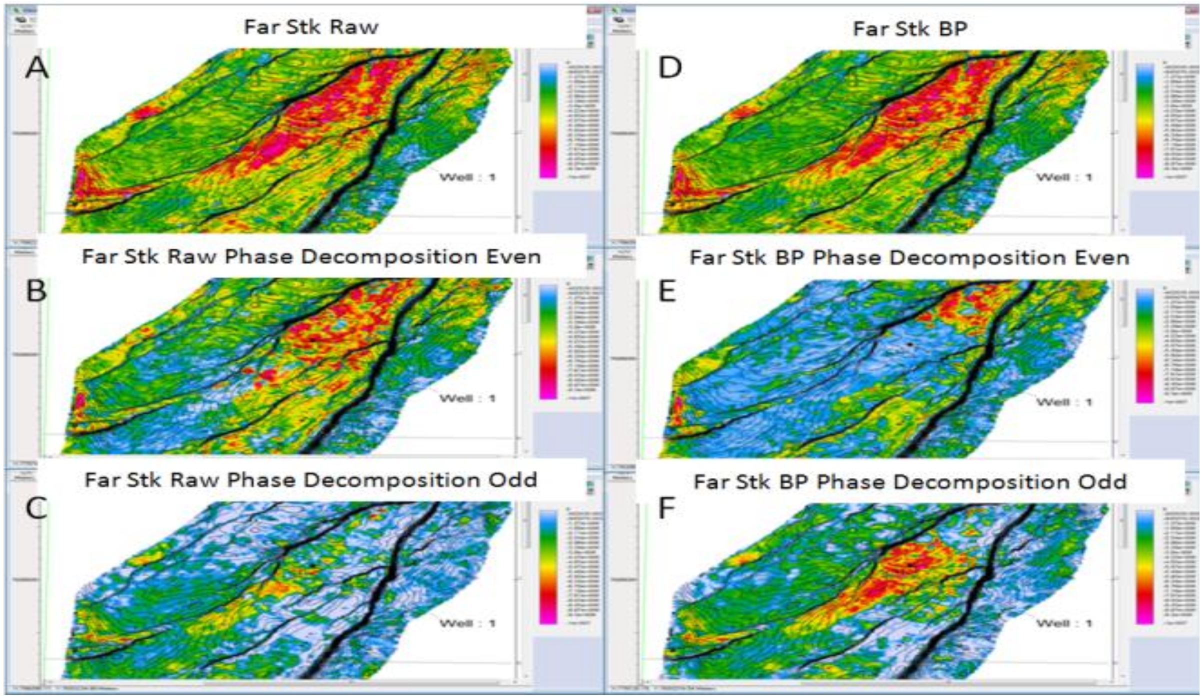

Figure 6. Map extraction for Event-1. Panels A through C show extraction at original frequency bandwidth data, and D through F at bandpass filtered data. Panel E (even) and F (odd) clearly show the separation of amplitudes into phase components, where the pay section of the reservoir is separated by a normal fault. Time contours are overlain.

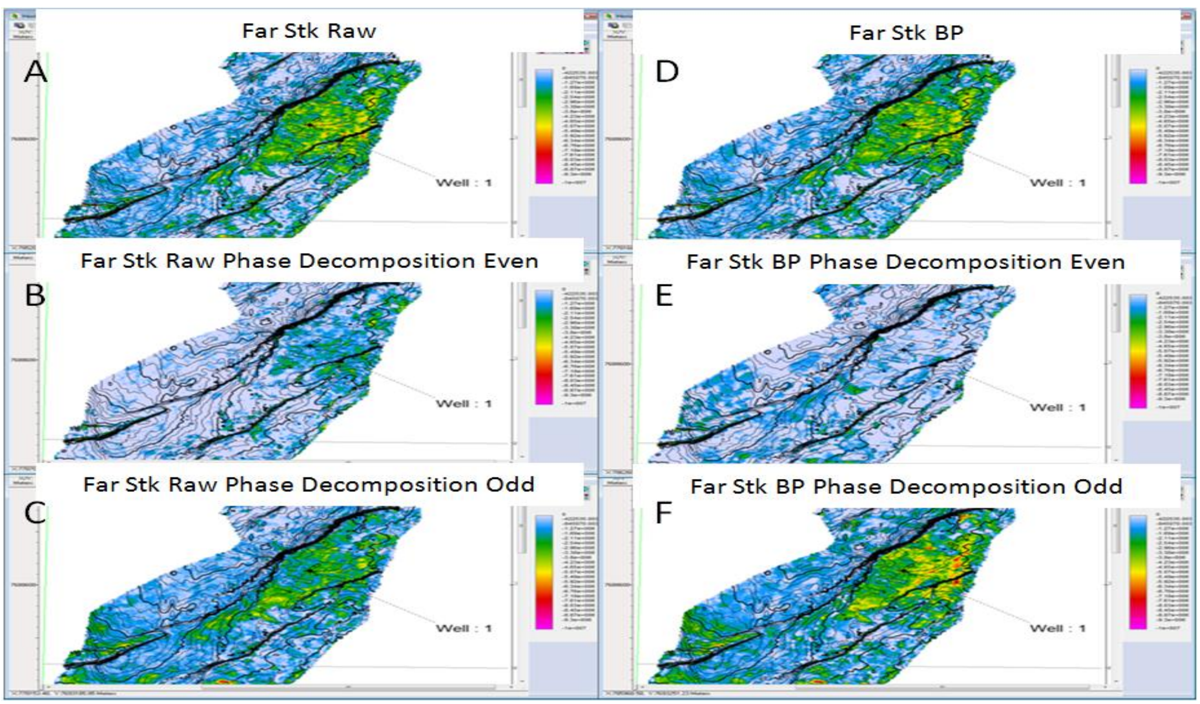

Figure 7. Map extraction for Event-2. Panels A through C show extraction at original frequency bandwidth data, and D through F at bandpass filtered data. Panel E (even) and F (odd) clearly show the separation of amplitudes into phase components.

References

Castagna, J.P., and S. Sun, 2006, Comparison of spectral decomposition methods: First Break, Volume 24.

Castagna, J.P., Oyem, A., Portniaguine, O., and Aikulola, U., 2016, Phase Decomposition: Interpretation, in press